3766 *Biochemistry* **2010,** *49,* 3766–3773
DOI: 10.1021/bi100232q

BIOCHEMISTRY
including biophysical chemistry & molecular biology
Article

Biochemical and Structural Characterization of *Mycobacterium tuberculosis* β-Lactamase with the Carbapenems Ertapenem and Doripenem†

Lee W. Tremblay,‡ Fan Fan,‡ and John S. Blanchard*

Department of Biochemistry, Albert Einstein College of Medicine, 1300 Morris Park Avenue, Bronx, New York 10461.
‡*These authors contributed equally to this work.*

Received February 15, 2010; Revised Manuscript Received March 29, 2010

ABSTRACT: Despite the enormous success of β-lactams as broad-spectrum antibacterials, they have never been widely used for the treatment of tuberculosis (TB) due to intrinsic resistance that is caused by the presence of a chromosomally encoded gene (*blaC*) in *Mycobacterium tuberculosis*. Our previous studies of TB BlaC revealed that this enzyme is an extremely broad-spectrum β-lactamase hydrolyzing all β-lactam classes. Carbapenems are slow substrates that acylate the enzyme but are only slowly deacylated and can therefore act also as potent inhibitors of BlaC. We conducted the *in vitro* characterization of doripenem and ertapenem with BlaC. A steady-state kinetic burst was observed with both compounds with magnitudes proportional to the concentration of BlaC used. The results provide apparent K_m and k_{cat} values of 0.18 μM and 0.016 min^{-1} for doripenem and 0.18 μM and 0.017 min^{-1} for ertapenem, respectively. FTICR mass spectrometry demonstrated that the doripenem and ertapenem acyl−enzyme complexes remain stable over a time period of 90 min. The BlaC−doripenem covalent complex obtained after a 90 min soak was determined to 2.2 Å, while the BlaC−ertapenem complex obtained after a 90 min soak was determined to 2.0 Å. The 1.3 Å diffraction data from a 10 min ertapenem-soaked crystal revealed an isomerization occurring in the BlaC−ertapenem adduct in which the original Δ^2-pyrroline ring was tautomerized to generate the Δ^1-pyrroline ring. The isomerization leads to the flipping of the carbapenem hydroxyethyl group to hydrogen bond to carboxyl O2 of Glu166. The hydroxyethyl flip results in both the decreased basicity of Glu166 and a significant increase in the distance between carboxyl O2 of Glu166 and the catalytic water molecule, slowing hydrolysis.

Tuberculosis (TB),[1] caused by *Mycobacterium tuberculosis*, continues to be a worldwide health concern (*1*). There were an estimated 9.3 million new cases of TB in 2007 and approximately 1.3 million HIV-negative patient fatalities as well as nearly half a million deaths among HIV-positive populations (*2*). Even 50 years after the introduction of powerful antibiotics for treating TB, it has been estimated that one person is infected in the world every few seconds (*3*). The failure to control TB is due to the emergence of *M. tuberculosis* strains that are multiply drug resistant toward the front line antimycobacterial drugs such as isoniazid and rifampicin.

As one of the most important antibiotic families, β-lactams include a broad range of molecules such as penicillin derivatives, cephalosporins, monobactams, carbapenems, and β-lactamase inhibitors. The carbapenems exhibit the broadest spectrum of activity among the β-lactam antimicrobials, providing safe and efficacious therapies in the treatment of serious infections caused by Gram-positive, Gram-negative, and anaerobic bacterial pathogens (*4*, *5*). Carbapenem antibiotics were originally developed from thienamycin, a natural product identified in culture filtrates of *Streptomyces cattleya* (*6*). There are four carbapenems approved thus far for human use: imipenem, meropenem, ertapenem, and doripenem (*5*). Imipenem was the first carbapenem approved by the U.S. Food and Drug Administration (FDA) in 1985 and is by far the most widely used carbapenem. The use of meropenem was approved in 1995, followed by ertapenem and doripenem in 2001 and 2007, respectively. Except for imipenem, all carbapenems are stable against the mammalian kidney dehydropeptidase (*7*). In clinical usage, imipenem and meropenem have to be given frequently to maintain high circulating levels. Also, weight-dosage adjustment of imipenem is required to minimize the chance of seizures (*8*). Ertapenem and doripenem can be given once per day due to their high target affinity and circulating stability (*5*, *9*). The smaller effective doses of these latter drugs reduce potential side effects, as well as the development of resistance (*10*). Currently, ertapenem and doripenem are used for complicated intra-abdominal and urinary tract infections (*11*, *12*).

Despite the general success of β-lactam antibiotics, they have not been widely used for the treatment of TB because of intrinsic resistance that is caused by the presence of a chromosomally encoded gene (*blaC*) in *M. tuberculosis* for a Class A Ambler β-lactamase (BlaC). Like other Class A β-lactamases, BlaC catalyzes the opening of the β-lactam ring via nucleophilic attack by an active site serine residue to generate the acyl−enzyme intermediate, followed by the hydrolysis of the ester bond to generate the ring-opened, inactive product. Our previous

†This work was supported in part by a grant from the National Institutes of Health (AI33696 to J.S.B.) and in part by the Charles Revson Foundation (to L.W.T.).
*To whom correspondence should be addressed. Phone: (718) 430-3096. Fax: (718) 430-8565. E-mail: blanchar@aecom.yu.edu.
[1]Abbreviations: BlaC, *M. tuberculosis* β-lactamase; TB, tuberculosis; XDR-TB, extensively drug resistant; rmsd, root-mean-square deviation.

 Published on Web 03/30/2010

studies of TB BlaC revealed that this enzyme is an extremely broad-spectrum β-lactamase hydrolyzing all β-lactam classes, including the carbapenems meropenem and imipenem (*13*). Being slow substrates that exhibit rapid acylation followed by a slow deacylation step, meropenem and imipenem also act as potent inhibitors of BlaC (*14*). FTICR mass spectrometry demonstrated that the acylated intermediate remains stable for many minutes (*14*). Such slow turnover rates allowed the determination of the three-dimensional structure of BlaC in complex with meropenem at a resolution of 1.8 Å. *In vivo* studies showed that meropenem in combination with the β-lactamase inhibitor, clavulante, is bactericidal against clinical TB strains that are phenotypically extensively drug resistant (XDR-TB) (*14*). As an extension of our prior work, we conducted an *in vitro* characterization of doripenem and ertapenem with BlaC.

MATERIALS AND METHODS

All chromatographic materials were purchased from Pharmacia. Meropenem and faropenem were from IKT Laboratories. Doripenem (as Doribax) was from Ortho-McNeil Pharmaceutical Inc. (Raritan, NJ). Ertapenem (as Invanz) was from Merck&Co. Inc. The potassium salt of clavulanic acid was from Sigma Aldrich. All other chemicals were purchased from Sigma or Aldrich. Nitrocefin was purchased from Beckton Dickinson.

Purification of BlaC. Recombinant and truncated BlaC from *M. tuberculosis* was expressed from plasmid pET28a(+) and purified to homogeneity as described by Hugonnet and Blanchard (*13*).

Kinetics. The steady-state rate of hydrolysis of the β-lactam ring was monitored as a decrease in the absorbance in the UV region, as described previously (*13*). Assays using doripenem, ertapenem, faropenem, and meropenem were performed at 296 nm (ε = 7540 M^{-1} cm^{-1}), 295 nm (ε = 9970 M^{-1} cm^{-1}), 306 nm (ε = 3445 M^{-1} cm^{-1}), and 297 nm (ε = 6152 M^{-1} cm^{-1}), respectively. Assays using the chromogenic substrate nitrocefin were performed at 486 nm (ε = 20500 M^{-1} cm^{-1}). Assays were performed in 100 mM MES (pH 6.5). Reactions were initiated by the addition of enzyme at concentrations between 0.1 and 25 μM using 100 μM carbapenem substrate.

Inhibition Studies. Carbapenems at concentrations ranging from 0.1 to 10 μM were tested as inhibitors of 1.5 nM BlaC using 60 μM nitrocefin as a substrate. Time courses were followed for 15 min. For slow onset inhibition, reaction velocities as a function of time were fitted to eq 1:

$$[P] = v_s t + \frac{v_i - v_s}{k_{iso}}[1 - \exp(-k_{iso} t)] \quad (1)$$

where [P] is the concentration of the product, v_i and v_s are the initial and final reaction velocities, respectively, for the reaction in the presence of inhibitor, k_{iso} is the apparent first-order rate constant for the interconversion between v_i and v_s, and t is time.

The general mechanism can be modeled as

$$E + S \underset{k_{-1}}{\overset{k_1}{\rightleftharpoons}} E \cdot S \xrightarrow{k_2} E - S \xrightarrow{k_3} E + P \quad (2)$$

where k_1 and k_{-1} represent the rates of reversible binding of carbapenem to and dissociation of carbapenem from BlaC, respectively, k_2 represents the rate of irreversible cleavage of the carbapenem β-lactam ring, and k_3 represents the rate of hydrolysis of the BlaC−-carbapenem adduct.

For this model, the rate constant that describes k_{iso} is given by eq 3, where K_d equals k_{-1}/k_1.

$$k_{iso} = k_3 + \frac{k_2[I]}{K_d + [I]} \quad (3)$$

In eq 4, the K_m value can be expressed as

$$K_m = \frac{K_d k_3}{k_2 + k_3} \quad (4)$$

In addition, from the determined k_2 and k_3 values, k_{cat} is calculated from eq 5, assuming k_2 and k_3 are much less than k_1 and k_{-1}.

$$k_{cat} = \frac{k_2 k_3}{k_2 + k_3} \quad (5)$$

Mass Spectrometry. All mass spectra were recorded on a 9.6 T Fourier transform ion cyclotron resonance (FTICR) mass spectrometer (Ionspec, Lake Forest, CA). To avoid salt interference, BlaC was dialyzed against 20 mM ammonium bicarbonate (pH 6.5). The molecular mass of each protein sample was determined for the +25 charge state using the equation $m = (m/z \times 25) - 25$ on the isotopic centroid. To monitor the intermediate of steady-state turnover or small molecular mass spectrometry, 51 μM enzyme was incubated with 25 μM carbapenem in a total volume of 20 μL. An aliquot of 1 μL was withdrawn at the desired times (0, 30, 60, and 90 min) and mixed with 9 μL of a mixing solution (containing 50% acetonitrile and 0.1% formic acid). The resulting mixture was injected into the FTICR mass spectrometer.

Crystallization. BlaC was crystallized in the hanging drop vapor diffusion configuration over well conditions that included 0.1 M HEPES (pH 7.5) and 2 M $NH_4H_2PO_4$. The final pH of the well solution was 4.1. Protein at a concentration of 10 mg/mL was mixed 1:1 with the well solution and incubated at 18 °C. Initial crystals grew within a week but were small, sparse, and amorphous. New wells were sealed and allowed to equilibrate overnight. Equilibrated drops were microseeded, which resulted in efficient crystal growth as well as improved morphology. Iterative seeding resulted in diffraction quality crystals of the active enzyme.

Data Collection and Refinement. Crystals were soaked with either ~50 mM ertapenem or doripenem in mother liquor with 20% glycerol as a cryoprotectant. Data were collected after 10 and 90 min soaks with ertapenem and a 90 min soak with doripenem at Brookhaven National Laboratory on beamlines X12C and X29, in which various resolutions of diffraction were obtained depending on the soaking times and beamline. The data were processed using either HKL2000 (*15*) or Mosflm (*16*). Our previous structure of clavulanate-bound *M. tuberculosis* β-lactamase (*17*) [Protein Data Bank (PDB) entry 3CG5] was used to phase all the data, using the CCP4 software suite (*18*). Iterative rounds of structural refinement and model building were performed in Refmac5 (*19*, *20*) and Coot (*21*). Table 1 lists the data collection statistics for the structures as well as the final refinement statistics.

RESULTS AND DISCUSSION

Kinetics. The accurate determination of the kinetic parameters for doripenem and ertapenem was severely hampered by apparent very low K_m values, very low k_{cat} values, and the modest extinction coefficients accompanying hydrolysis. At the BlaC

Table 1: Data Collection and Refinement Statistics[a]

	doripenem Δ^1-isomer[b]	ertapenem Δ^2-isomer	ertapenem Δ^1-isomer
	Data Collection		
resolution (Å)	50.0−2.2 (2.32−2.20)	50.0−1.30 (1.33−1.30)	50.0−2.0 (2.07−2.00)
completeness (%)	100 (100)	100.0 (100)	99.5 (99.9)
redundancy	7.6 (7.4)	7.5 (5.7)	4.4 (4.4)
$I/\sigma(I)$	3.8 (1.6)	21.4 (1.8)	9.8 (4.0)
R_{merge}	0.077 (0.47)	0.057 (0.757)	0.158 (0.373)
space group	$P2_12_12_1$	$P2_12_12_1$	$P2_12_12_1$
unit cell	a = 49.99 Å	a = 49.66 Å	a = 49.93 Å
	b = 68.07 Å	b = 67.92 Å	b = 67.83 Å
	c = 75.79 Å	c = 75.55 Å	c = 75.20 Å
	$\alpha = \beta = \gamma$ = 90.0°	$\alpha = \beta = \gamma$ = 90.0°	$\alpha = \beta = \gamma$ = 90.0°
no. of reflections	13695 (1943)	60263 (4388)	17920 (1762)
	Refinement		
R_{work}	0.161 (0.176)	0.147 (0.265)	0.175 (0.191)
R_{free}	0.205 (0.237)	0.176 (0.278)	0.222 (0.281)
average B factor (Å^2)			
protein	6.97	10.49	6.09
adduct	27.32	18.64	15.50
solvent	17.51	32.64	14.36
PO_4	12.89	14.40	10.53
rmsd			
bonds (Å)	0.010	0.010	0.012
angles (deg)	1.204	1.428	1.386
Ramachandran plot			
favored	97.7%	97.7%	98.1%
outliers	0.0%	0.0%	0.0%
PDB entry	3IQA	3M6B	3M6H

[a]Values in parentheses are for the highest-resolution bin. [b]These data processed using Mosflm.

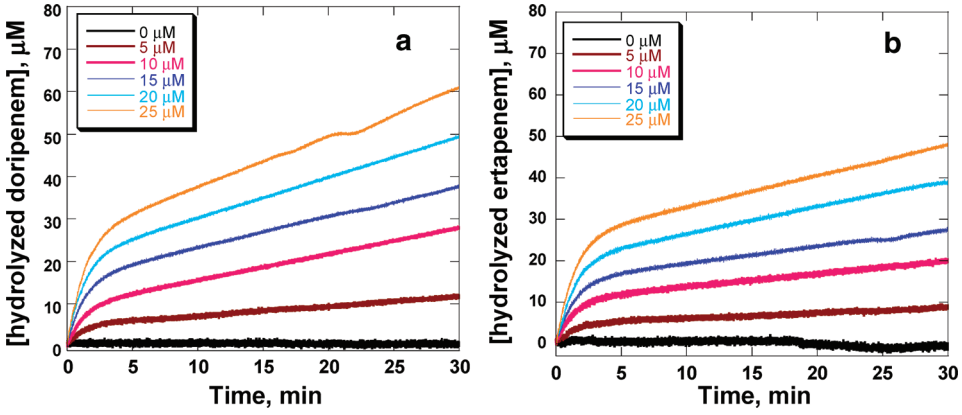

FIGURE 1: Time courses of doripenem (A) and ertapenem (B) hydrolysis with various concentrations of BlaC.

concentration required to see any significant rate of reaction (~2 μM), variation of the doripenem or ertapenem concentration from 2 to 20 μM yielded almost no difference in rate, suggesting their K_m values were $< 2\,\mu$M. The steady-state kinetic parameters determined for faropenem, a structurally distinct penem, were as follows: $K_m = 55 \pm 11\,\mu$M, and $k_{cat} = 0.65 \pm 0.04$ min^{-1} (data not shown). This K_m value is ~17 times larger and the k_{cat} value 8 times faster than those of meropenem (*14*).

Detailed investigations of the kinetics of carbapenem hydrolysis under near-stoichiometric enzyme concentrations were conducted over 30 min time periods. As shown in Figure 1, a steady-state kinetic burst was observed with both compounds where the magnitudes of the burst are proportional to the concentration of BlaC used. Extrapolation of the rates of hydrolysis to the y-axis demonstrates that the acylation is stoichiometric with the enzyme concentration.

Because of the extremely feeble turnover rate, we further tested these carbapenems as inhibitors of the reaction of nitrocefin with BlaC. Nitrocefin is an extremely good substrate for BlaC, and its β-lactam ring-opened form is extremely chromogenic. As shown in Figure 2, doripenem and ertapenem acted as slow-onset, tight binding inhibitors of BlaC when the hydrolysis of nitrocefin was monitored. In contrast, faropenem exhibited standard, competitive inhibition with no time-dependent component (data not shown). This type of time-dependent inhibition for a dead-end inhibitor is modeled as being due to the reversible formation of a noncovalent complex (E−I), followed by the reversible conversion to an isomerized complex (E−I*). However, in the case of

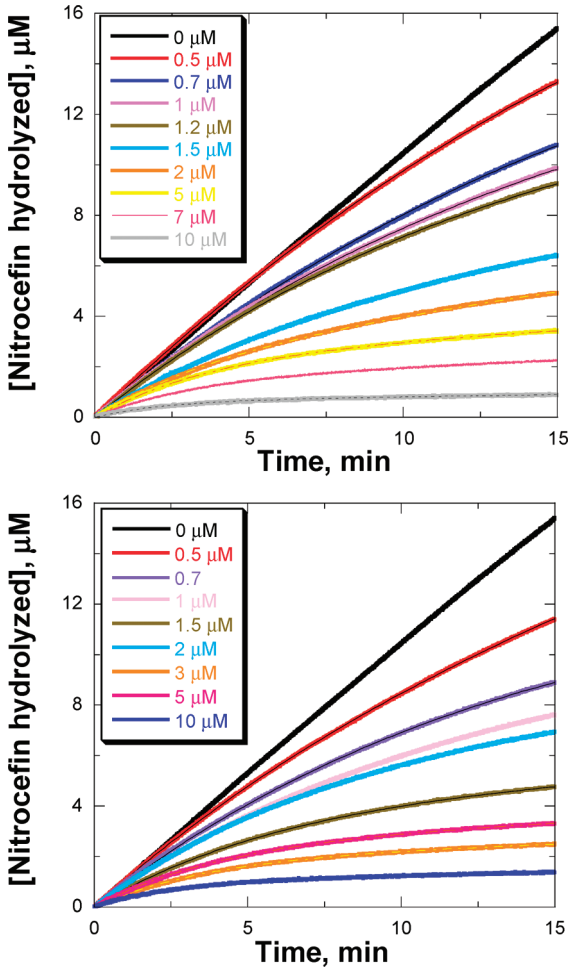

FIGURE 2: Time courses of nitrocefin hydrolysis by BlaC in the presence of doripenem (top) and ertapenem (bottom).

a slow substrate for BlaC, the initially formed Michaelis complex reacts with the enzyme in an irreversible step to generate the BlaC−carbapenem covalent intermediate. This is then hydrolyzed slowly to regenerate the free enzyme that can react with nitrocefin. While the same equation is used to fit the two models, the kinetic constants that contribute to k_{iso} (Figure S1 of the Supporting Information) and K_i (or K_d) are different. Using the fits of the slow-onset data and eq 3 to calculate K_d, k_2, and k_3, we can then use eqs 4 and 5 to calculate the apparent K_m and k_{cat} values for doripenem (0.18 μM and 0.016 min^{-1}, respectively) and ertapenem (0.18 μM and 0.017 min^{-1}, respectively). We have not corrected for the concentration of nitrocefin used in these experiments because of the large standard errors (>40%) associated with these kinetic parameters (the reported K_m values are apparent values). However, the extremely tight binding and extremely slow turnover of these carbapenems are evident from these rather imprecise kinetic data.

Mass Spectrometry. The rapid acylation and slow deacylation of BlaC by the carbapenems allow the observation of the covalently bound, acyl−enzyme intermediate by Fourier transform ion cyclotron resonance. A freshly prepared solution containing excess BlaC and doripenem displayed three peaks: the first peak corresponding to free BlaC with a mass/charge ratio (m/z) of 28785.0, a second peak corresponding to the covalently acylated BlaC−doripenem complex with a mass/charge ratio (m/z) of 29204.1, and a third peak whose mass corresponds to the mass of the covalently acylated BlaC−doripenem complex minus 44 mass units (m/z 29161.0) (as shown in Figure 3). With ertapenem, the two covalent acylated BlaC complex peaks observed had molecular weights of 29260.0 and 29217.1, corresponding to the acylated BlaC−ertapenem complex and the acylated BlaC−doripenem complex minus 44 mass units, respectively. These data demonstrate that both doripenem and ertapenem undergo the same chemical breakdown in the active site as meropenem (*14*). Once the acyl−enzyme intermediate forms, the carbapenems partition between hydrolysis and enzyme-catalyzed decomposition of the C6 hydroxyethyl substituent, via a retro-Aldol decomposition, which yields acetaldehyde (*14*). Intriguingly, the intensities of the acyl−enzyme complexes remain stable over the time period of 90 min for doripenem and ertapenem. This is in contrast with previous observations with meropenem, where the levels of the acylated forms of the enzyme started to diminish after several minutes. These data suggest that doripenem and ertapenem form more stable complexes with BlaC than meropenem, reinforcing the kinetic data.

X-ray Crystallography. The 2.2 Å data from a 90 min doripenem-soaked crystal were refined to an R_{work} of 0.161 and an R_{free} of 0.205. The 1.3 Å diffraction data from a 10 min ertapenem-soaked crystal refined to an R_{work} of 0.147 and an R_{free} of 0.176. The 2.0 Å diffraction data from a 90 min ertapenem-soaked crystal were refined to an R_{work} of 0.175 and an R_{free} of 0.222. In these three structures, the active site Ambler residue Ser70 has been covalently linked with the ring open form of these β-lactams in accordance with the acylation chemistry of the first half of the enzymatic reaction (Scheme 1). The quality of the electron density is displayed in Figures 4 and 5 under the calculated $F_o - F_c$ omit maps contoured at 2.0 σ.

The C3 atoms of the pyrroline rings of doripenem and ertapenem covalent adducts are sp^3 hybridized in the 90 min soaks. These results require an isomerization event occurring in the BlaC−carbapenem adducts in which the original Δ^2-pyrroline ring is tautomerized to generate the Δ^1-pyrroline ring, evidenced by the collinear positioning of the C5, N1, C2, and C3 atoms. In addition, the BlaC−doripenem and −ertapenem covalent adduct densities allow for the positioning of the thioether sulfur atom in the unambiguous assignment of the *S* configuration at C3, requiring protonation at the *re* face of the C2=C3 bond. This result is similar to our earlier findings with BlaC crystals soaked with meropenem on similar time scales (*14*) and represents the thermodynamically preferred product with the *trans* orientation of the C4 methyl and thioether substituents. Interestingly, the recently reported structure of the Class D β-lactamase, OXA-1 covalent adduct with doripenem, revealed that while an identical isomerization had taken place, the final Δ^1-pyrroline ring product was of the opposite, *R*, stereochemistry (*22*).

In the structure determined after the shorter 10 min soak, the BlaC−ertapenem adduct was covalently bound in the active site, but in a different geometry. On this shorter time scale, the BlaC−ertapenem adduct C3 atom is found in its original sp^2 hybridization, with the definitive collinear positioning of the thioether sulfur atom in line with the N1, C2, C3, and C4 bonds indicating the presence of the Δ^2-pyrroline ring. This result requires that β-lactam ring cleavage and isomerization of the methyl pyrroline ring not be concerted.

The active site interactions vary in some subtle ways between the pre- and postisomerization ertapenem complexes, yet a number of common interactions are observed in all complexes. Both the BlaC−ertapenem and −doripenem adducts bind as

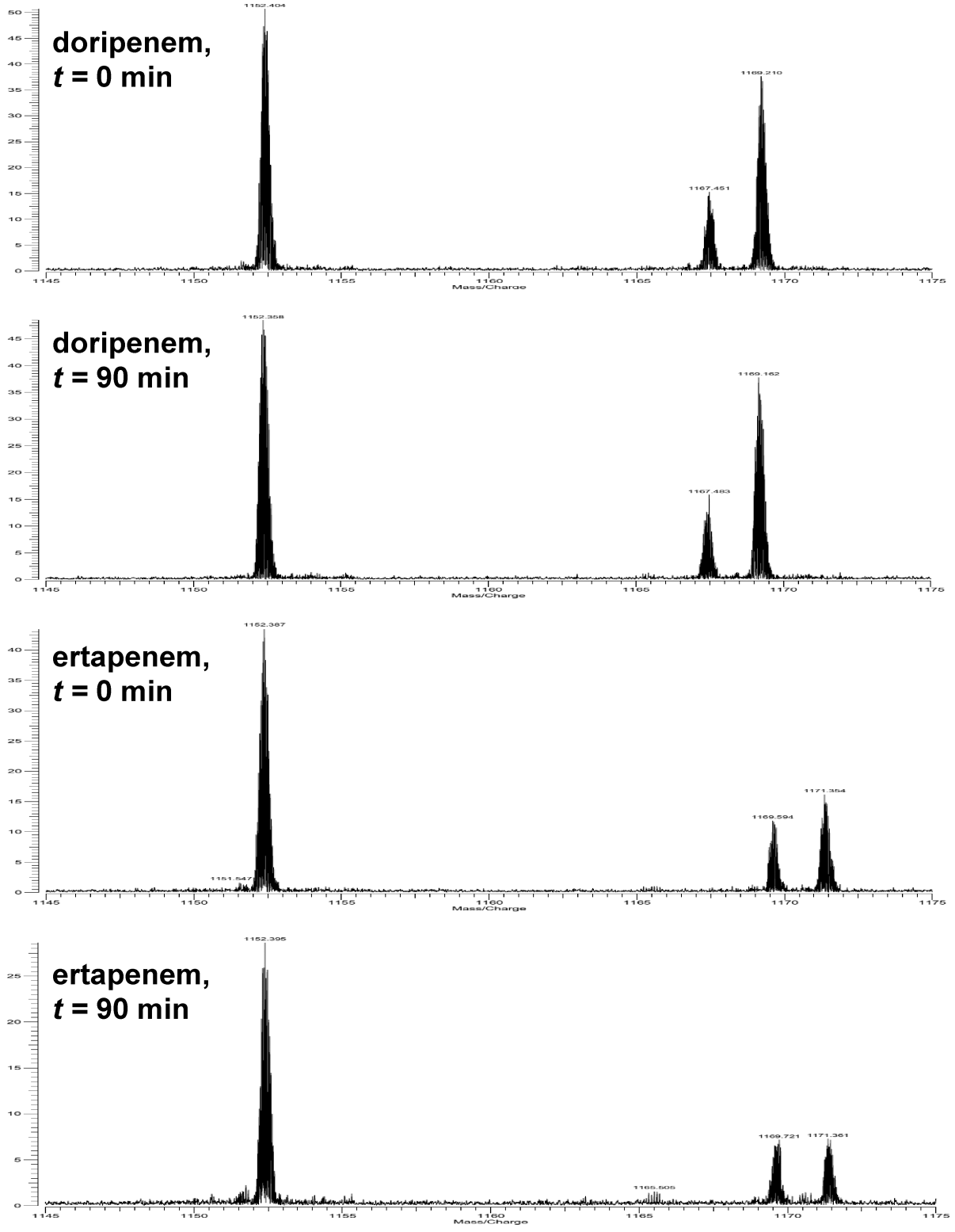

FIGURE 3: Mass spectra of enzyme−carbapenem species. The +25 charge-state ions are shown.

covalent adducts with the active site Ser70 and position their lactam ring-opened ester carbonyl oxygen atom within the oxyanion hole formed from hydrogen bonding interactions with the Ser70 and Thr253 amide nitrogen atoms. All structures contain a hydrophobic interaction between the methyl group of the pyrroline ring and the side chain of Ile117 and different forms of hydrogen bonding interactions between the C6 hydroxyethyl substituent of the carbapenem and Glu166. All three structures also exhibit a conserved interaction between the side chain hydroxyl of Ser130, which consistently forms a hydrogen bond with the pyrroline ring nitrogen atom at a distance of 2.7−2.8 Å. The pyrroline C2 carboxylate group forms hydrogen bonds with the Thr251 hydroxyethyl side chain and an active site water molecule. In structures of other β-lactamase−carbapenem adducts, this carboxylate electrostatically interacts with a conserved arginine residue (R244 in TEM-1) (*23*), but this is not the case for BlaC. In the preisomerized ertapenem structure, there is an additional hydrogen bond between the C2 carboxylate of the

Scheme 1: (A) Structures of Doripenem and Ertapenem and (B) Chemical Mechanism of Hydrolysis of Ertapenem by *M. tuberculosis* BlaC

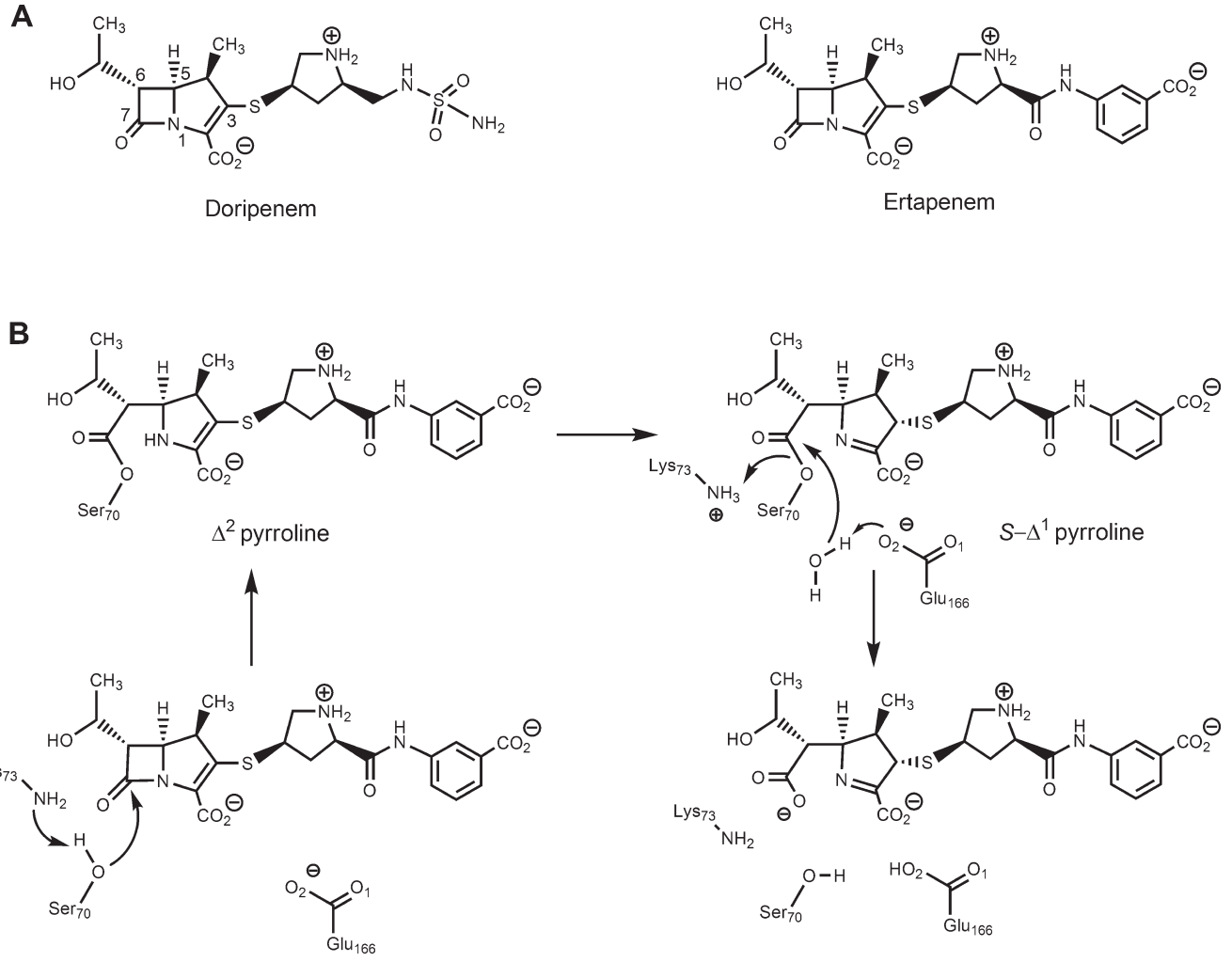

pyrroline ring and Thr253, which is broken when the *m*-aminobenzoate "arm" observed in the postisomerized ertapenem structure is repositioned. The isomerization and stereospecific protonation lead to a reorientation of the terminal portion of the molecule within the active site, allowing for the formation of the hydrogen bond between the terminal carboxylate group of the *m*-aminobenzoic acid moiety and Ser118. A final difference between the initially formed Δ^2-pyrroline isomer and the final Δ^1-pyrroline form is the orientation of the C6 hydroxyethyl substituent. In the preisomerized complex, it is oriented away from Lys73 and forms a hydrogen bond to the carboxyl O1 atom of Glu166 as well as the Asn186 nitrogen but rotates upon isomerization to form a hydrogen bond with the carboxyl O2 atom of Glu166 and the ε-amino group of Lys73 in a manner similar to that observed for the doripenem complex.

The structures of the pre- and postisomerization states reveal the mechanistic basis for the relative stability of the carbapenems within the active site of BlaC and their ability to resist hydrolysis by the enzyme. As seen in Scheme 1, deacylation hydrolysis from the enzyme requires the activation of the conserved active site water by the side chain carboxyl O2 atom of Glu166. The probability of water activation by Glu166 decreases with the increased distance between the two. The distance between the carboxyl O2 atom of Glu166 and the active site water is significantly increased after isomerization from 2.4 to 2.7 Å, making water activation less probable. The isomerization event does not directly cause these changes but rather alters the positioning of the adduct such that the adduct hydroxyethyl flips in the active site, breaking the hydrogen bond formed between the hydroxyl group with the side chain amide nitrogen of Asn186 and the adjacent carboxyl O1 atom of Glu166. The hydroxyethyl substituent then rotates to generate a hydrogen bond network with Lys73 and the carboxyl O2 atom of Glu166, effectively "pulling" this essential base away from the conserved active site water. These residues (Lys73 and Glu166) are involved as general bases in the acylation and deacylation reactions, respectively. In addition, by forming a hydrogen bond with the carboxyl O2 atom of Glu166, the reoriented hydroxyethyl substituent reduces the basicity of Glu166. These two factors, introduced in the reorientation of the hydroxyethyl substituent in the postisomerization complex, reduce the level of water activation and thereby stabilize the acyl intermediate in the active site. The studies reported here allow us to directly visualize the changes that occur between the pre- and postisomerization adduct structures and provide atomic-level observations relevant to the biphasic kinetics previously reported for the reactions between carbapenems and the RTEM β-lactamase (*24*).

The Δ^2- to Δ^1-pyrroline isomerized forms of carbapenems have been known to form within the active sites of various β-lactamase enzymes (*25*). Confirming this, crystal structures of

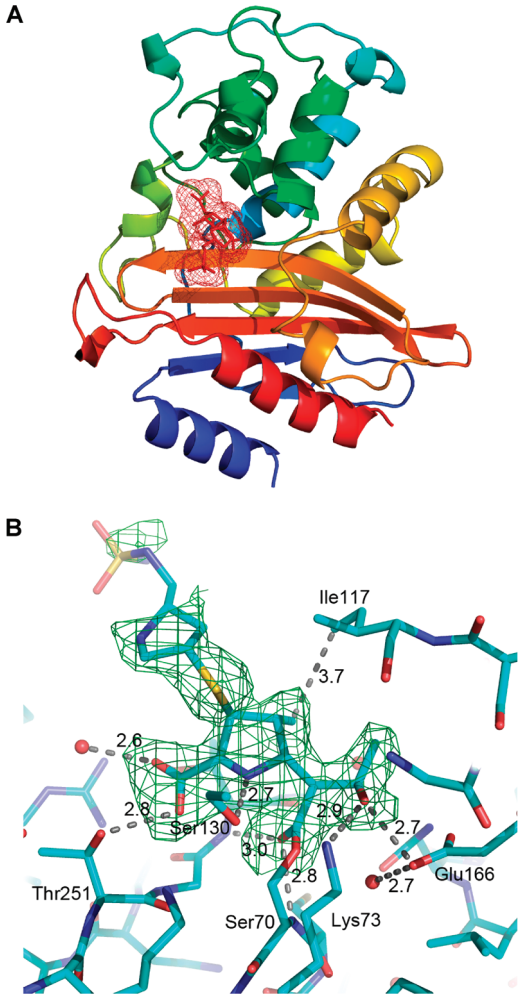

FIGURE 4: (A) Overall structure of BlaC displayed in rainbow from the N-terminus (blue) to the C-terminus (red), with the doripenem adduct displayed in red surface mesh. (B) $F_o - F_c$ omit density (green) contoured at 2.0σ surrounds the covalent doripenem adduct formed at the Ambler active site residue serine 70. All structure figures were produced using Pymol.

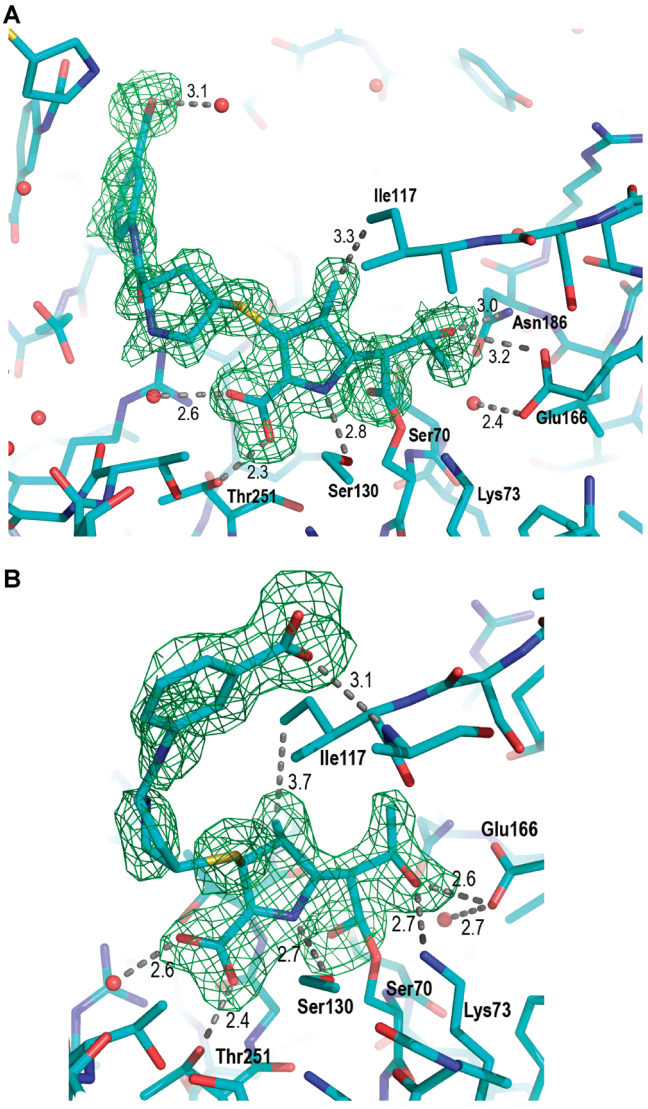

FIGURE 5: (A) $F_o - F_c$ omit density (green) contoured at 2.0σ surrounds the covalent ertapenem adduct formed at the Ambler active site residue serine 70 in the preisomerization state. (B) $F_o - F_c$ omit density (green) contoured at 2.0σ surrounds the covalent ertapenem adduct formed at the Ambler active site residue serine 70 in the postisomerization state. The resolution of the densities unambiguously demonstrates the shift in stereochemistry with the change from sp^2 to sp^3 hybridization of the carbapenem C3 atom with the change in the position of the density associated with the *m*-aminobenzoate and the hydoxyethyl ertapenem moieties.

carbapenems bound within the active sites of the Class A β-lactamases TEM-1 (PDB entry 1BT5) (*26*) and SHV-1 (PDB entry 2ZD8) (*27*) as well as AmpC (PDB entry 1LL5) (*28*), a Class C β-lactamase, all revealed the Δ^2 form of the carbapenem bound in the active sites, while the Class D OXA-1 (PDB entry 3ISG) (*22*) and the Class A BlaC (PDB entry 3DWZ) (*14*) were both bound with carbapenems in the Δ^1 isomerized forms with *R* and *S* stereochemistries, respectively. Our findings are the first to show the structures of both the Δ^2 and Δ^1 forms of a carbapenem bound to a single β-lactamase. Interestingly, several of the structures of carbapenems bound as the Δ^2 isomers show evidence for alternate conformations for the carbapenem carbonyl oxygen position. This oxygen is found buried within the oxyanion hole as well as bound in a position rotated by 180°, usually facing an opposing serine residue (Ser130). In these instances, it has been proposed that the flipping of the carbonyl oxygen from the oxyanion hole blocks formation of the deacylation tetrahedral intermediate to inhibit the enzyme. In the cases of OXA-1 and BlaC, the carbapenem carbonyl oxygen is found bound tightly only within the oxyanion hole and no evidence of alternate conformers has been observed. In these cases, inhibition by the carbapenem is likely due to disruption of water activation.

A second possible reason for the observed alternate conformers at the carbapenem carbonyl is likely the position of the carbapenem carboxylate moiety within those active sites. To date, those β-lactamases with alternate conformations for the carbapenem carbonyl have a highly conserved Arg244 reside that electrostatically interacts with the carbapenem carboxylate moiety. The OXA-1 and BlaC active sites lack this arginine interaction and instead use a combination of threonine and/or serine residues coordinated with waters to bind the carboxylate moiety. These residues are located closer to the oxyanion hole and act to "clamp" the carboxylate into a proximal position, as opposed to the Arg244 mechanism of carboxylate binding, in which distance introduces flexibility, allowing for the alternate positioning of the pyrroline ring. This pattern of bonding to the carbapenem allows for alternate "in/out" conformations of the carbapenem carbonyl in the oxyanion hole. In contrast, the carbapenem carbonyl is

tightly bound in the oxyanion hole in BlaC in both the Δ^2 and Δ^1 forms reported here.

SUPPORTING INFORMATION AVAILABLE

Dependence of k_{burst} on ertapenem concentration and doripenem concentration (Figure S1). This material is available free of charge via the Internet at http://pubs.acs.org.

REFERENCES

1. Dye, C., Floyd, K., Uplekar, M., Bierrenbach, A., Bergstrom, K., Blanc, L., Grezmska, M., Gunneberg, C., Lonnroth, K., Nunn, P., Pantoja, A., Raviglione, S., and Weyer, K. (2008) Global tuberculosis control: Surveillance, planning, financing: WHO report 2008, World Health Organization, Geneva.
2. Bauquerez, R., Blanc, L., Bierrenbach, A., Brands, A., Ciceri, K., Falzon, D., Floyd, K., Glaziou, P., Gunneberg, C., Hiatt, T., Hosseini, M., Pantoja, A., Uplekar, M., Watt, C., and Wright, A. (2009) Global Tuberculosis Control: Epidemiology, Strategy, Financing: WHO Report 2009, World Health Organization, Geneva.
3. Netto, E. M., Dye, C., and Raviglione, M. C. (1999) Progress in global tuberculosis control 1995−1996, with emphasis on 22 high-incidence countries. Global Monitoring and Surveillance Project. *Int. J. Tuberc. Lung Dis. 3*, 310–320.
4. Mandell, L. (2009) Doripenem: A new carbapenem in the treatment of nosocomial infection. *Clin. Infect. Dis. 49* (Suppl. 1), S1–S3.
5. Baughman, R. P. (2009) The use of carbapenems in the treatment of serious infections. *J. Intensive Care Med. 24*, 230–241.
6. Birnbaum, J., Kahan, F. M., Kropp, H., and MacDonald, J. S. (1985) Carbapenems, a new class of β-lactam antibiotics. Discovery and development of imipenem/cilastatin. *Am. J. Med. 78*, 3–21.
7. Livermore, D. M. (2001) Of *Pseudomonas*, porins, pumps and carbapenems. *J. Antimicrob. Chemother. 47*, 247–250.
8. Calandra, G., Lydick, E., Carrigan, J., Weiss, L., and Guess, H. (1988) Factors predisposing to seizures in seriously ill infected patients receiving antibiotics: Experience with imipenem/cilastatin. *Am. J. Med. 84*, 911–918.
9. Bhavnani, S. M., Hammel, J. P., Cirincione, B. B., Wikler, M. A., and Ambrose, P. G. (2005) Use of pharmacokinetic-pharmacodynamic target attainment analyses to support phase 2 and 3 dosing strategies for doripenem. *Antimicrob. Agents Chemother. 49*, 3944–3947.
10. Lynch, M. J., Drusano, G. L., and Mobley, H. L. (1987) Emergence of resistance to imipenem in *Pseudomonas aeruginosa*. *Antimicrob. Agents Chemother. 31*, 1892–1896.
11. Behera, B., Mathur, P., Das, A., and Kapil, A. (2009) Ertapenem susceptibility of extended spectrum β-lactamase-producing Enterobacteriaceae at a tertiary care centre in India. *Singapore Med. J. 50*, 628–632.
12. Paterson, D. L., and Depestel, D. D. (2009) Doripenem. *Clin. Infect. Dis. 49*, 291–298.
13. Hugonnet, J. E., and Blanchard, J. S. (2007) Irreversible inhibition of the *Mycobacterium tuberculosis* β-lactamase by clavulanate. *Biochemistry 46*, 11998–12004.
14. Hugonnet, J. E., Tremblay, L. W., Boshoff, H. I., Barry, C. E., III, and Blanchard, J. S. (2009) Meropenem-clavulanate is effective against extensively drug-resistant *Mycobacterium tuberculosis*. *Science 323*, 1215–1218.
15. Otwinowski, Z., and Minor, W. (1997) Processing of X-ray Diffraction Data Collected in Oscillation Mode. *Methods Enzymol. 276*, 307–326.
16. Leslie, A. G. W. (1992) Mosflm. Joint CCP4 + ESF-EAMCB Newsletter on Protein Crystallography No. 26.
17. Tremblay, L. W., Hugonnet, J. E., and Blanchard, J. S. (2008) Structure of the covalent adduct formed between *Mycobacterium tuberculosis* β-lactamase and clavulanate. *Biochemistry 47*, 5312–5316.
18. Potterton, E., Briggs, P., Turkenburg, M., and Dodson, E. (2003) A graphical user interface to the CCP4 program suite. *Acta Crystallogr. D59*, 1131–1137.
19. Murshudov, G. N., Vagin, A. A., and Dodson, E. J. (1997) Refinement of Macromolecular Structures by the Maximum-Likelihood Method. *Acta Crystallogr. D53*, 240–255.
20. Pannu, N. S., Murshudov, G. N., Dodson, E. J., and Read, R. J. (1998) Incorporation of prior phase information strengthens maximum-likelihood structure refinement. *Acta Crystallogr. D54*, 1285–1294.
21. Emsley, P., and Cowtan, K. (2004) Coot: Model-building tools for molecular graphics. *Acta Crystallogr. D60*, 2126–2132.
22. Schneider, K. D., Karpen, M. E., Bonomo, R. A., Leonard, D. A., and Powers, R. A. (2009) The 1.4 Å crystal structure of the class D β-lactamase OXA-1 complexed with doripenem. *Biochemistry 48*, 11840–11847.
23. Zafaralla, G., Manavathu, E. K., Lerner, S. A., and Mobashery, S. (1992) Elucidation of the role of arginine-244 in the turnover processes of class A β-lactamases. *Biochemistry 31*, 3847–3852.
24. Easton, C. J., and Knowles, J. (1982) Inhibition of the RTEM β-lactamase from *Escherichia coli*. Interaction of the enzyme with derivatives of olivanic acid. *Biochemistry 21*, 2857–2862.
25. Kalp, M., and Carey, P. R. (2008) Carbapenems and SHV-1 β-lactamase form different acyl-enzyme populations in crystals and solution. *Biochemistry 47*, 11830–11837.
26. Maveyraud, L., Mourey, L., Kotra, L. P., Pedelacq, J., Guillet, V., Mobashery, S., and Samama, J. (1998) Structural Basis for Clinical Longevity of Carbapenem Antibiotics in the Face of Challenge by the Common Class A β-Lactamases from the Antibiotic-Resistant Bacteria. *J. Am. Chem. Soc. 120*, 9748–9752.
27. Nukaga, M., Bethel, C. R., Thomson, J. M., Hujer, A. M., Distler, A., Anderson, V. E., Knox, J. R., and Bonomo, R. A. (2008) Inhibition of class A β-lactamases by carbapenems: Crystallographic observation of two conformations of meropenem in SHV-1. *J. Am. Chem. Soc. 130*, 12656–12662.
28. Beadle, B. M., and Shoichet, B. K. (2002) Structural basis for imipenem inhibition of class C β-lactamases. *Antimicrob. Agents Chemother. 46*, 3978–3980.